AXIAL–GAP ELECTROSTATIC MICROMOTOR

Anca TOMESCU, Sorin ANTONIU, F.M.G. TOMESCU
Electrical Engineering Dept., POLITEHNICA University – Bucharest
Ramona Marilena TOADER
ICPE COENERG – Bucharest

The torque–versus–angle mechanical characteristic of an one–sided axial–gap electrostatic motor is calculated by an approximate analytical method and by a finite element numerical method.

INTRODUCTION

Multiple applications in industry, medicine, military, and many other fields make microdevices and micromotors a subject of increasing interest. In particular, electrostatic motors [1,2,3,4,5] appear to be more convenient than motors of a classical type, based on electromagnetic forces, as the structure of microdevices is generally subjected to certain restrictions derived from the manufacturing process which uses integrated circuit technology. The one–sided axial–gap electrostatic micromotor, where a salient–pole rotor is revolving above the stator poles deposited on an insulator substrate, [6], is another simple realization.

A preliminary performance evaluation is extremely useful in the design of micromotors, with a view to establish the range of the proper design and manufacturing requirements. In this respect, the evaluation of the mechanic characteristic of the micromotor, i.e., the dependence of the active torque on the rotation angle of the rotor, is of foremost importance for both the overall performance evaluation and the design of appropriate driving procedures. The present paper aims at the computation of an approximate mechanic characteristic of the one–sided axial–gap micromotor, obtained under some reasonable simplifying assumptions.

DEVICE MODEL AND SIMPLIFYING ASSUMPTIONS

The micromotor under study, [6], consists in a stator with 8 insulated poles deposited on an insulating substrate, and a rotor with 6 salient–poles, revolving above the stator (fig. 1). The operation of the motor is quite simple: the conducting rotor is permanently in contact with the zero potential revolving axis, while appropriate stator poles are successively placed at a driving potential V. The energized stator pole attracts the nearest rotor pole until the latter reaches a symmetric position with respect to the former, and thus makes the rotor rotate. By adequately energizing successive stator poles, the rotor can sustain a continuous revolving movement.

Some simplifying hypotheses are supposed to apply:

1°. The axial airgap is negligible with respect to the radii of the stator and rotor pole faces;

2°. The width of the deposited stator poles is negligible with respect to the axial airgap and the rotor width;

3°. The insulating substrate is linear, homogeneous, without volume charge or electrical polarization distributions.

The motor structure is characterized by: $\alpha = \pi/3$ – the rotor pole pitch, $\beta = \pi/6$ – the angular pole width (for both stator and rotor), $\gamma = \pi/4$ – the stator pole pitch, $\delta = \pi/6$ – the rotor inter–pole angle, $\varepsilon = \pi/12$ – the stator inter–pole angle, h – the rotor clearance above the stator, g – the rotor axial width, R_1 – the inner stator pole radius, R_2 – the outer rotor and stator pole radius, $\varepsilon = 4.1$ – the *relative* permittivity of the insulating substrate.

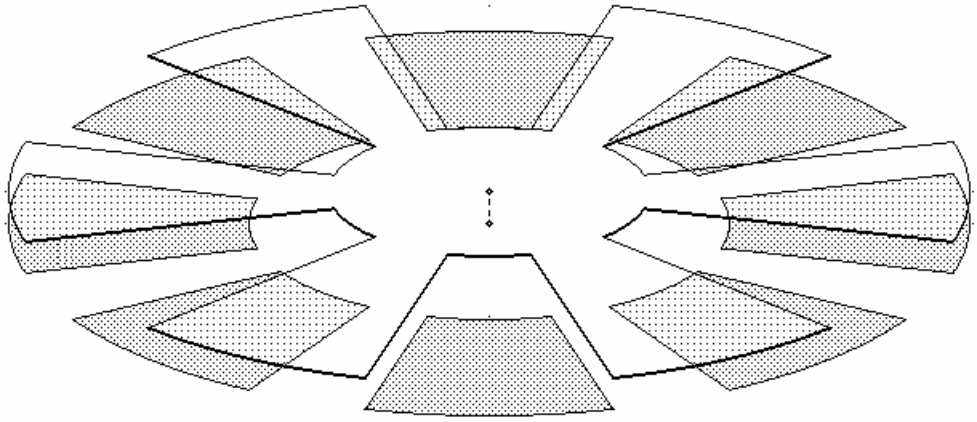

Fig. 1. Device model

The rotational symmetry of the motor structure makes it sufficient the study of its mechanic characteristic over an $\alpha/2 = \pi/6$ angle, between two symmetric configurations of null electric torque. The starting configuration is that where two rotor poles are symmetrically placed with respect to the energized stator pole, and the final configuration is that where a rotor pole is face–to–face with the energized stator pole. Moreover, according to the simplifying hypotheses, for any given radius, the angular distribution of the electrostatic field can be approximated as a two–dimensional plane–parallel distribution. Subsequently, the radial variation of the field structure can be approximated as a set of such plane–parallel field distributions at successive radii, followed by an approximate Gauss quadrature [7] of the relevant computed values. Finally, the stray electric field distribution along the inner and outer stator circumferences can be approached as a two–dimensional axial electrostatic field distribution in axial planes. Each of these two problems is studied analytically by the field line approximation method and by a finite element numerical method.

The active electric torque is computed as [8,9,10]

$$T = \frac{\partial W^*}{\partial \theta} = \frac{\partial}{\partial \theta} \frac{C V^2}{2} \bigg|_{V=\text{ct.}} = \frac{V^2}{2} \frac{\partial C(\theta)}{\partial \theta} \quad ,$$

where W^* is the electric co–energy, V is the potential of the energized stator pole, θ is the rotor position angle, i.e., the angle between the symmetry planes of the approaching rotor pole and the energized stator pole, and $C(\theta)$ is the rotor–stator capacitance.

ANALYTICAL COMPUTATION OF THE MECHANIC CHARACTIRISTIC

The computation of the electric torque is reduced to the computation of the electric rotor–stator capacitance as a function of the rotation angle θ.

In accordance with the simplifying assumptions, the analytical treatment of the angular distribution of the electric field is approximated as a plane–parallel distribution,

where the rotor performs a local translation movement with respect to the stator. The spectrum of the field lines, approximated by straight segments and circular arcs, [11] , changes when the rotor moves, so that five different field line patterns, separated by four limiting cases, have to be considered for field lines starting from the stator inferior face and five other for field lines starting from the stator superior face. Moreover, the relative position of the limiting cases changes with the calculation radius, which multiplies the number of angle intervals with different field line pattern and computation formulae to be considered. As an example, for the relatively simple (fifteenth) field line pattern represented in fig. 2, the capacitance per unit length results as

$$C_{\mathrm{XV}} = \varepsilon_0 \left[\frac{L(\beta+\theta)}{h} + \frac{\varepsilon}{\pi} \ln\left(1+\frac{\pi x_1}{\varepsilon h}\right) + \frac{\varepsilon}{\pi(\varepsilon+1)} \ln \frac{h-\pi x_1+\pi x_2(\varepsilon+1)/\varepsilon}{h+\pi x_1/\varepsilon} + \right.$$
$$\left. + \frac{\varepsilon}{\pi} \ln \frac{d-\alpha x_2+\pi(2L-x_3)}{d-\alpha x_2+\pi x_2} + \frac{\varepsilon}{\pi} \ln\left(1+\frac{\pi x_3}{\varepsilon h}\right) + \frac{1}{\pi} \ln\left(1-\frac{\pi\theta R}{h}\right) \right] \quad ,$$

for

$$-\frac{\beta}{2}\cos\alpha_1 \le \theta \le \frac{h}{\pi R} - \frac{\beta}{2\pi\varepsilon} \quad , \quad \text{where} \quad \sin\alpha_1 - \alpha_1\cos\alpha_1 = \frac{\varepsilon h}{L} \quad ,$$

with $R = R_0$ the current radius, and

$$L = R\beta \quad , \quad x_1 = -R\theta \quad , \quad x_3 = \frac{L(2\pi-1)+d-\alpha_2 x_2}{2\pi} \quad , \quad d = L\sin\alpha_2 \quad ,$$

$$x_2 = L\cos\alpha_2 \quad , \quad \text{where} \quad \sin\alpha_2 - \cos\alpha_2(\alpha_2+\pi\varepsilon) = \frac{\varepsilon(h-\pi x_1)}{L} \quad .$$

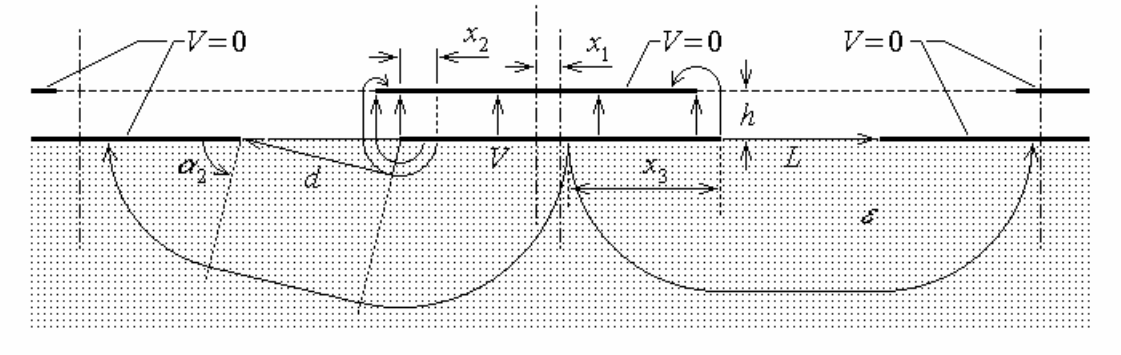

Fig. 2. Approximate field line pattern in transverse planes

Under the same simplifying assumptions, the analytical treatment of the electric field problem associated with the field lines in axial planes (fig. 3) remains to apply to the stray field lines only, and add the small correction of the capacitance per unit length

$$C_A = \frac{\varepsilon\varepsilon_0}{\pi} \left\{ \ln\left[1+\frac{\pi(R_2-R_1)}{\varepsilon(\varepsilon+2)h}\right] + \frac{1}{\varepsilon+1} \ln\left[1+\frac{\pi(\varepsilon+1)(R_2-R_1)}{\varepsilon(\varepsilon+2)h}\right] \right\} \quad .$$

The capacitance resulted from the plane–parallel angular problem, completed with the correction given by the axial problem, was assembled, according to formulae like those above, for three radii needed in the 3–point Gauss approximate integration, for 16 different cases and 96 angular positions within the $\pi/6$ range. The resulted capacitance–versus–angle variation was then smoothed by a sliding average procedure [12] with a 4 entries half–range (fig. 4).

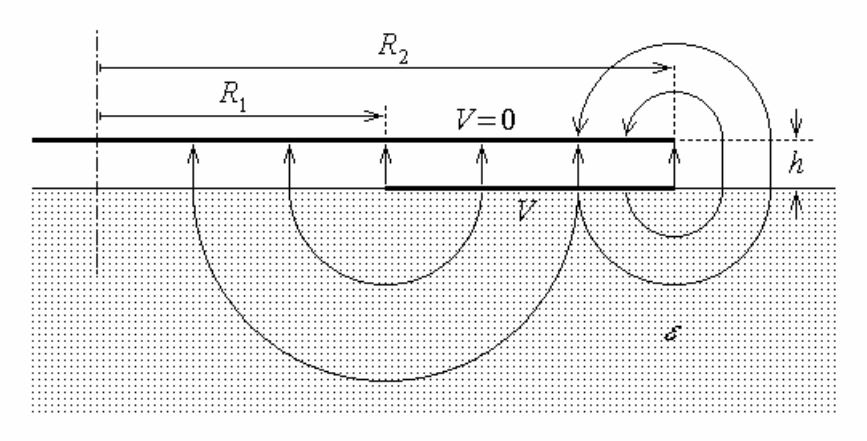

Fig. 3. Approximate field line pattern in axial planes

The approximate mechanic characteristic torque–versus–rotation angle was readily computed, according to the above given formula, by using an approximate derivation formula [7], and was followed, here again, by a smoothing procedure based on a sliding average technique with a 10 entries half–range (fig. 4).

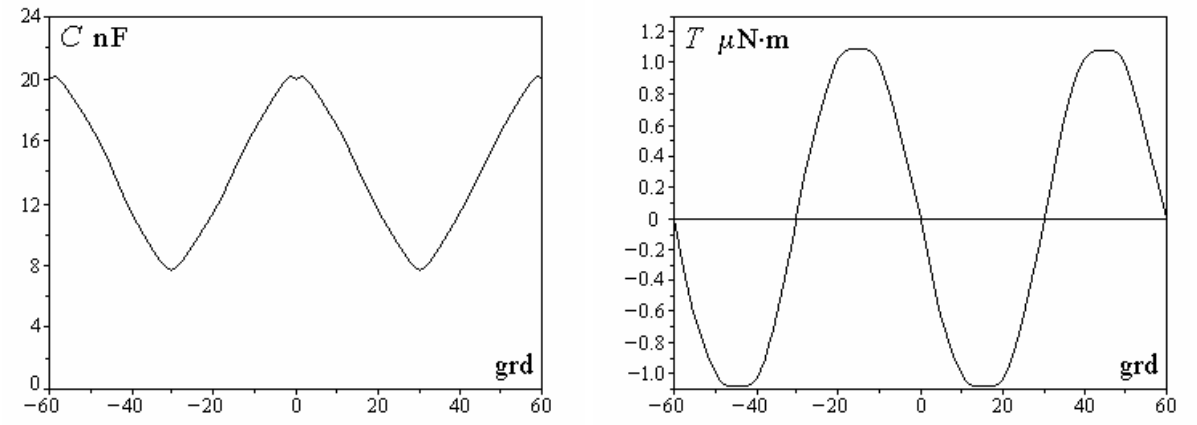

Fig. 4. Capacitance and torque – analytical computation

NUMERICAL COMPUTATION OF THE MECHANIC CHARACTERISTIC

In the plane–parallel electrostatic field problem, associated with the angular field distribution, the electric potential decreases very rapidly from the energizing V value to zero, so that the same $\pi/6$ sector only of the motor, with the energized stator axis at the middle, is sufficient to be studied by the finite element numerical approach, [6], with boundary conditions corresponding to the applied potentials on conductors and null Neumann conditions on the remaining boundary. The capacitance per unit length is determined, both in

terms of electric charge and in terms of electric energy for each radius needed in the approximate Gauss integration,

$$R_m = R_0 - \frac{R_2 - R_1}{2\sqrt{3}} \quad , \quad R_0 = \frac{R_1 + R_2}{2} \quad , \quad R_M = R_0 + \frac{R_2 - R_1}{2\sqrt{3}} \quad ,$$

seven values between $-30°$ and $0°$, with a $5°$ step are considered for the rotor–stator angle.

The axial electrostatic field problem, associated with field lines in axial planes, gives the capacitance for the entire cylindrical structure of the given axial cross–section. It is quite difficult to extract from it the contribution of the electric field in the radial rotor–stator airgap, so that the solution is more useful as a confirmation of the analytical computations.

The results of the numerical modelling were processed, for the indicated angular positions, in a similar manner to that of the analytical approach, for both the capacitance–versus–angle dependence and for the torque–versus–angle dependence, i.e., the mechanic characteristic (fig. 5).

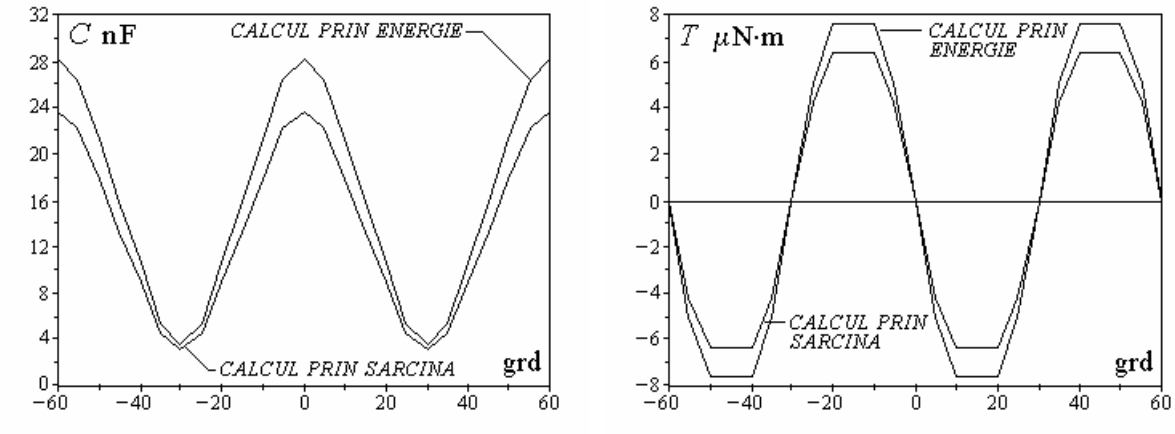

Fig. 5. Capacitance and torque – numerical computation

The usual mechanic characteristic torque–versus–revolving speed can then be derived with reference to a particular driving procedure, aiming at relating the revolving speed with the switching rate of the energized pole pairs.

CONCLUSIONS

The approximate mechanic characteristic of a radial–gap salient–pole electrostatic motor was calculated, under reasonable simplifying hypotheses. The computations done by using an analytical and a numerical method are in a satisfactory agreement, and allow a valuable evaluation of the motor performance, preliminary to the proper design of the device.

The results presented here are also in good agreement with published results [1], reported for the same constructive data.

ACKNOWLEDGEMENTS

Thanks are due to the staff of the Numerical Methods Laboratory, and to colleagues in the Group of Theoretical Electrical Engineering of the Electrical Engineering Department, "Politehnica" University of Bucharest.

REFERENCES

1. M.P. Omar, M. Mehregany, R.L. Mullen, *Electric and Fluid Field Analysis of Side–Drive Micromotors*, IEEE JMEMS, Vol 1, No. 3, September 1992, pp. 130–140.
2. R. Legtenberg, E. Berenscholt, J. van Baar, M. Elwenspoek, *An Electrostatic Lower Stator Axial – Gap Polysilicon Wobble Motor Part I* : *Design and Modeling*, IEEE JMEMS, Vol. 7, No. 1, March 1998, pp. 79–86.
3. R. Legtenberg, E. Berenscholt, J. van Baar, M. Elwenspoek, *An Electrostatic Lower Stator Axial – Gap Polysilicon Wobble Motor Part II* : *Fabrication and Performance*, IEEE JMEMS, Vol. 7, No. 1, March 1998, pp. 87–93.
4. V.D. Samper, A.J. Sangster, R.L. Reuben, U. Wallrabe, *Multistator LIGA–Fabricated Electrostatic Wobble Motors with Integrated Synchronous Control*, IEEE JMEMS, Vol. 7, No. 2, June 1998, pp. 214–223.
5. A.J. Sangster, V.D. Samper, *Accuracy Assessment of 2–D and 3–D Finite–Element Models of a Double Stator Electrostatic Wobble Motor*, IEEE JMEMS, Vol.6, No.2, June 1997, pp. 142–150.
6. Ramona Marilena Toader, *Micromotor electrostatic cu interstitiu axial*, Graduation thesis, Department of Electrical Engineering, Polytechnic University of Bucharest, 2004.
7. Anca Tomescu, I.B.L. Tomescu, F.M.G. Tomescu, *Modelarea numericã a câmpului electromagnetic*, MatrixRom, Bucharest, 2003.
8. J. Van Bladel, *Electromagnetic Fields*, McGraw-Hill Book Company, New York, 1964.
9. H.A. Haus, J.R. Melcher, *Electromagnetic Fields and Energy*, Prentice Hall, Englewood Cliffs, J.J., 1989.
10. Anca Tomescu, F.M.G. Tomescu, R. Mãrculescu, *Bazele electrotehnicii – Câmp electromagnetic*, MatrixRom, Bucharest, 2002.
11. Anca Tomescu, F.M.G. Tomescu, *Bazele electrotehnicii – Sisteme electromagnetice* (*Lecture Notes*), Department of Electronics and Telecommunications, Polytechnic University of Bucharest, 1996.
12. Anca Tomescu, F.M.G. Tomescu, *Transmisia informatiei* (*Lecture Notes*), Department of Electrical Engineering, Polytechnic University of Bucharest, 1999.